

State-to-State Dynamics Analysis of the F + CHD₃ Reaction: A Quasiclassical Trajectory Study

Joaquín Espinosa-García* and José L. Bravo

Departamento de Química Física, Universidad de Extremadura, 06071 Badajoz, Spain

Received: November 27, 2007; Revised Manuscript Received: March 11, 2008

An exhaustive state-to-state dynamics study was performed to analyze the F + CHD₃ → FD(*v'*, *j'*) + CHD₂(*v*) gas-phase abstraction reaction. Quasiclassical trajectory (QCT) calculations, including corrections to avoid zero-point energy leakage along the trajectories, were performed at different collision energies on an analytical potential energy surface (PES-2006) recently developed by our group. Whereas the CHD₂ coproduct appears vibrationally and rotationally cold, most of the available energy appears as FD(*v'*) product vibrational energy, peaking at *v'* = 2 and *v'* = 3, with the population in the latter level growing as the energy increases. The excitation function rises from the threshold of the reaction and then levels off at higher energies, with the maximum contribution from the FD(*v'* = 3) level. The state-specific FD(*v'*) scattering distributions correlated with the coproduct CHD₂ in the *v*₄ = 2 and *v*₃ = 1 states, at different collision energies, show a steady change from backward to forward scattering as the energy increases. This similar behavior for the two coproduct vibrational states, *v*₄ = 2 and *v*₃ = 1, agrees qualitatively with the experimental measurements. Comparison with theoretical and experimental results for the isotopic analogues, F + CH₄ and F + CD₄, shows that the title reaction presents a direct mechanism, similar to the perdeuterated reaction, but contrasts with that of the F + CH₄ reaction. These results for the dynamics of different isotopic variants, always in qualitative and sometimes in quantitative agreement with experiment, show the capacity of the PES-2006 surface to correctly describe the title reaction, even though there are differences that could be due to deficiencies of the PES but also to the known limitations of the classical treatment in the QCT method.

1. Introduction

The quest for an accurate potential energy surface (PES) for the hydrogen-abstraction reaction of fluorine atoms with methane and its isotopic analogues has a long history in our research group. In 1996, we reported¹ the first analytical potential energy surface for the polyatomic F(²P) + CH₄ → FH(*v'*) + CH₃ reaction (PES-1996), which was modified and updated in 2005² to correct its most obvious deficiencies (PES-2005). This latter surface was symmetric with respect to any permutation of the four methane hydrogen atoms, and was calibrated to reproduce the experimental rate coefficients. Shortly after we had constructed PES-2005, two dynamics studies using quasiclassical trajectory (QCT) calculations^{3,4} questioned its suitability for describing the dynamics of this reaction and pointed out four major drawbacks of PES-2005. First, the energy drop along the reaction path in the product valley did not reproduce *ab initio* calculations. Second, the surface neglected the FH...CH₃ van der Waals minimum in this product valley. Third, PES-2005 showed much less FH(*v'*) vibrational excitation than seen in experiments, and fourth, the FH(*v'*) rotational distribution was considerably hotter than that found by experiment. To correct the deficiencies of PES-2005, we recently⁵ constructed a new analytical potential energy surface for the title reaction, denoted PES-2006.

With this surface, we performed an exhaustive study⁵ of the F(²P) + CH₄ → FH(*v'*) + CH₃ reaction, including the kinetics using variational transition-state theory (VTST) with semiclassical transmission coefficients and the dynamics using quasiclassical trajectory (QCT) calculations. For the latter, we

considered the zero-point-energy (ZPE) question along the trajectories, i.e., the problem of how to handle the quantum mechanical ZPE in a classical mechanics simulation. We concluded that the agreement with experiment (always qualitative and sometimes quantitative) lended confidence to the results obtained using PES-2006. A very sensitive test of the accuracy of the PES is the study of Feshbach-type scattering resonances in the F(²P) + CH₄ → FH(*v'*) + CH₃ reaction, because these are quantum mechanical phenomena and their description requires great detail in the construction of the PES. Experimental values for these resonances were recently reported by Shiu et al.,⁶ who used a rotating-source crossed-beam apparatus. We studied⁷ these resonances theoretically using the reduced-dimensionality rotating-line-umbrella (RLU) quantum scattering model on the PES-2006, in hyperspherical coordinates. We concluded that the wells found in the hyperspherical adiabats, the oscillatory pattern in the cumulative and state-to-state reaction probabilities, the forward/backward predominance in the differential cross section at a collision energy of 1.8 kcal mol⁻¹, and the dramatic change of the scattering angle with energy were related to scattering resonances and assigned them to a quasibound complex on the vibrationally adiabatic ground-state potential.

To more fully understand this reaction and the role of isotopic substitution, one of us recently performed QCT dynamics calculations of the F + CD₄ → FD(*v'*, *j'*) + CD₃(*v*, *j*) reaction using the same PES-2006⁸ and compared the results with recent experimental work by Liu et al.,^{9–12} who studied this reaction exhaustively using the time-sliced ion velocity imaging technique to obtain the state-specific correlation of coincident product pairs. The calculations showed a steady change of the

* To whom correspondence should be addressed. E-mail: joaquin@unex.es.

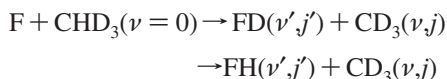
TABLE 1: Stationary-Point Properties

	CHD ₃	SP	CHD ₂	FD
		harmonic vibrational frequencies (cm ⁻¹) ^a		
	3106 (2993) ^b (ν_1)	3096	3149 (3114) ^c (ν_1)	2983 (2998) ^e
	2313 (2263) (ν_4)	2306	2368 (2358) (ν_5)	
	2313 (2263) (ν_4)	2252	2233 (2187) (ν_2)	
	2155 (2142) (ν_2)	2083	1268 (1248) (ν_6)	
	1305 (1291) (ν_5)	1300	1021 (1006) (ν_3)	
	1305 (1291) (ν_5)	1231	497 (431) (555) ^d (ν_4)	
	1052 (1036) (ν_6)	1030		
	1052 (1036) (ν_6)	963		
	1027 (1003) (ν_3)	959		
		97		
		89		
		117 <i>i</i>		
ZPE (kcal/mol)	22.34	22.03	15.06	4.26
energies (kcal/mol) ^f				
ΔE_R	-28.22			
$\Delta H_R(0\text{ K})$	-31.23			
ΔE^\ddagger		+0.35		
$\Delta H^\ddagger(0\text{ K})$		+0.03		

^a Experimental or theoretical values in parentheses for comparison. ^b Experimental values from ref 31. ^c Theoretical values from ref 32. ^d Experimental values from ref 33. ^e Experimental values from ref 34. ^f ΔE_R and $\Delta H_R(0\text{ K})$ are the energy and enthalpy (0 K) of reaction, respectively; and ΔE^\ddagger and $\Delta H^\ddagger(0\text{ K})$ are the classical barrier height and the enthalpy of activation at 0 K, respectively.

scattering angle with collision energy, from backward scattering at low energies to forward scattering at high energies, which seems to indicate a direct mechanism for the F + CD₄ reaction. This signature not only reproduces the experimental information,¹¹ but is also markedly different from that obtained for the analogous F + CH₄ reaction,^{5,7} which seems to indicate that there are different mechanisms for the two isotopes.

Continuing with the analysis of the role of isotopic substitution, in the present work, we report a QCT dynamics study using the analytical PES-2006 surface of the reaction of fluorine atoms with trideuteromethane in its vibrational ground state, which can evolve along two channels, namely, D- and H-abstraction



Recently, Liu et al.¹³ performed an exhaustive experimental study of the D-abstraction reaction using the time-sliced ion velocity imaging technique to obtain the state-specific correlation of coincident product pairs. They analyzed the product scattering angular distribution (measured as the differential cross section, DCS) for different FD(ν') vibrational states correlated with two vibrational modes of the CHD₂ coproduct, $\nu_4 = 2$ and $\nu_3 = 1$. They found a highly inverted vibrational distribution of the FD(ν') product and a similar correlated vibrational branching ratio for the coproduct CHD₂ in the $\nu_4 = 2$ and $\nu_3 = 1$ modes. Because these experimental data can be used to test the accuracy of the recently developed PES-2006 surface, in the present work, we analyze only this D-abstraction reaction.

This article is structured as follows: In section 2, we briefly outline the potential energy surface and the computational details of the QCT calculations. The dynamics results are presented in section 3, along with comparisons of different dynamics properties with those for the analogous F + CH₄ and F + CD₄ reactions. Finally, section 4 presents the conclusions.

2. Potential Energy Surface and Computational Details

Recently, our group constructed a new PES for the gas-phase F + CH₄ → FH + CH₃ polyatomic reaction, PES-2006,⁵ which is symmetric with respect to the permutation of the methane hydrogen atoms, a feature that is especially interesting for

TABLE 2: Reaction Cross Section (σ) and Product Energy Partitioning at Different Collision Energies on the PES-2006 Surface

	1.5 kcal mol ⁻¹	2.8 kcal mol ⁻¹	8.0 kcal mol ⁻¹
σ (Å ²)	0.567	1.941	4.092
$f_V(\text{FD})$	0.71	0.69	0.64
$f_R(\text{FD})$	0.07	0.07	0.07
$f_V(\text{CHD}_2)$	0.08	0.08	0.08
$f_R(\text{CHD}_2)$	0.03	0.03	0.04
f_T	0.11	0.13	0.17

dynamics calculations. The functional form was developed in that work and therefore is not repeated here. Essentially, it consists of four London–Eyring–Polanyi (LEP) stretching terms, augmented by terms for out-of-plane bending and valence bending. In the calibration process, of the 32 parameters defining the PES, we fitted those required to reproduce the variation of the experimental thermal forward rate coefficients with temperature (as in earlier published work by our group) and the topology of the reaction from reactants to products. In the latter case, special care was taken in the reproduction of ab initio information along the reaction path (energies, geometries, and vibrational frequencies) and in the investigation of complexes in the entry and exit channels. Note that the consideration of the topology was an innovation with respect to earlier work.^{1,2}

Because there is abundant experimental information available for this reaction and its isotopic analogues, PES-2006 has been subjected to a great variety of tests, both kinetic and dynamic.^{5,7,8} Thus, from the kinetics point of view, the forward thermal rate coefficients calculated using variational transition-state theory (VTST) with semiclassical transmission coefficients agreed with experimental measurements, reproducing the Arrhenius plot. In addition, we found good agreement of the CH₄/CD₄ kinetic isotope effects (KIEs) at several temperatures—a very sensitive test of features of the new surface, such as barrier height and width, zero-point energy, and the tunneling effect. From the dynamics point of view, an extensive study employing quasi-classical trajectory (QCT) calculations was also performed on this surface. The theoretical results were found to reproduce (at least qualitatively) the available experimental information for a great variety of properties (total reaction cross section,

TABLE 3: QCT State-to-State Reaction Cross Section (σ_R) at Three Collision Energies on the PES-2006 Surface for the CHD₃($\nu = 0$) Reactant Ground State

product states	1.5 kcal mol ⁻¹		2.8 kcal mol ⁻¹		8.0 kcal mol ⁻¹	
	σ_R (Å ²)	percentage ^a	σ_R (Å ²)	percentage	σ_R (Å ²)	percentage
FD($\nu' = 2$) + CHD ₂ ($\nu_4 = 0$)	0.171	58	0.464	57	0.734	55
+ CHD ₂ ($\nu_4 = 1$)	0.085	29	0.237	29	0.374	28
+ CHD₂($\nu_4 = 2$)	0.030	10	0.083	10	0.133	10
+ CHD ₂ ($\nu_3 = 0$)	0.273	93	0.753	92	1.215	91
+ CHD₂($\nu_3 = 1$)	0.022	7	0.064	8	0.120	9
FD($\nu_4 = 0$) + CHD ₂ ($\nu_4 = 0$)	0.162	66	0.663	64	1.461	61
+ CHD ₂ ($\nu_4 = 1$)	0.061	25	0.286	28	0.599	25
+ CHD₂($\nu_4 = 2$)	0.019	8	0.065	6	0.144	6
+ CHD ₂ ($\nu_3 = 0$)	0.228	93	0.978	94	2.275	95
+ CHD₂($\nu_3 = 1$)	0.018	7	0.058	6	0.120	5

^a Percentage of the total reaction cross section for each channel. Differences from 100 for the sum in each channel are due to minor paths. In each channel, we separated the contributions for each CHD₂ vibrational state, ν_4 and ν_3 , to avoid double counting the FD contributions.

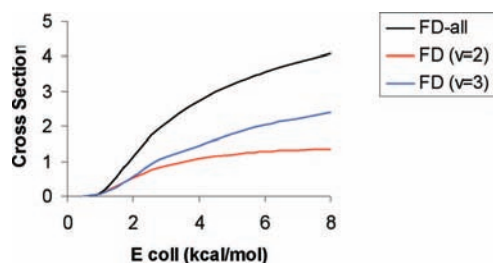


Figure 1. Excitation function (reaction cross section, in Å², versus the collision energy, in kcal mol⁻¹) for the F + CHD₃ → FD(ν') + CHD₂(ν) reaction obtained using the PES-2006 surface. The black line includes all FD vibrational states, and the red and blue lines correspond to the FD($\nu' = 2$) and FD($\nu' = 3$) levels, respectively.

product vibrational excitation, and differential cross section, among others). In sum, this agreement with experiment (always qualitative and sometimes quantitative) lent confidence to the results obtained using this PES-2006 polyatomic surface, although there were some differences that, of course, might be due to the PES itself, but also might be due to the known limitations of the QCT method (especially the treatment of the vibrational ZPE, i.e., the ZPE breakdown problem).

In the present work, QCT calculations^{14–16} were carried out using VENUS96 software,¹⁷ customized to incorporate our analytical PES. Moreover, a modification was included to compute the vibrational energy in each normal mode to obtain information on the CHD₂ coproduct vibrational distribution in the exit channel. Because VENUS96 freely rotates the molecules along the trajectories, the normal-mode energy calculation was preceded by a rotation of the molecule in order to maintain the orientation of the optimized geometry of the CHD₃ molecule for which the normal-mode analysis was being performed. Once this was done, a projection of the displacement and momentum matrices onto the normal-mode space allowed for the computation of the potential and kinetic energies for each normal mode. The energy in each harmonic normal mode was computed for the last geometry (coordinates and momenta) on the reactive trajectories. Because the harmonic approximation was used for this calculation, one could expect the procedure to break down for highly excited states. However, because we are interested in the lowest CHD₂ vibrational states, we can assume that this method is accurate enough for the present purpose. This approach was also used in earlier studies by our group^{5,8,18} with excellent results.

The accuracy of the trajectory was checked by the conservation of total energy and total angular momentum. The integration step was 0.01 fs, with an initial separation between the F atom and the CHD₃ molecule center of mass of 6.0 Å and a CHD₃ rotational energy of 20 K. The reagent collision energies considered in the present work ranged from 0.5 to 8.0 kcal mol⁻¹, and batches of 100 000 trajectories were calculated at each energy. The impact parameter, b , was sampled as $b = b_{\max}R^{1/2}$, with R being a random number in the interval [0, 1]. For all energies, we used the same maximum impact parameter, 3.5 Å, which was obtained at the highest energy. The maximum value of the impact parameter, b_{\max} , was obtained by calculating batches of 10 000 trajectories at fixed values of the impact parameter b and systematically increasing the value of b until no reactive trajectories were obtained.

A serious drawback of QCT calculations is related to the question of how to handle the quantum mechanical zero-point energy (ZPE) in a classical mechanics simulation.^{19–30} Many strategies have been proposed to correct for this quantum dynamical effect (see, for instance, refs 19–23 and 26 and references therein), but no completely satisfactory alternatives have emerged. Here, we employed a pragmatic solution, the so-called passive method,²³ by which all reactive trajectories that led to either a FD or a CHD₂ product with a vibrational energy below the respective ZPE were discarded. We call this approach histogram binning with double ZPE correction (HB-DZPE).

3. Results and Discussion

3.1. Stationary-Point Properties. The title reaction is a deuterium-abstraction reaction on trideuteromethane to yield the dideruteromethyl radical, with a slow change in the geometry of the nearly tetrahedral CHD₃ molecule to a planar geometry in CHD₂. The reactant and product properties (energies and vibrational frequencies) are listed in Table 1, and the enthalpy of reaction at 0 K is -31.23 kcal mol⁻¹. The saddle-point properties are, as expected, very similar to those of the F + CH₄ reaction.⁵ The transition state is “early”, i.e., it is a reactant-like transition state, in which the length of the bond that is being broken (C–D') increases by less than 1% and the length of the bond that is being formed (D'–F) is 94% greater than that in the products. The conventional transition-state enthalpy of activation at 0 K, $\Delta H_0^\ddagger = +0.03$ kcal mol⁻¹, is in good agreement with the values for the analogous F + CH₄ reaction.⁵

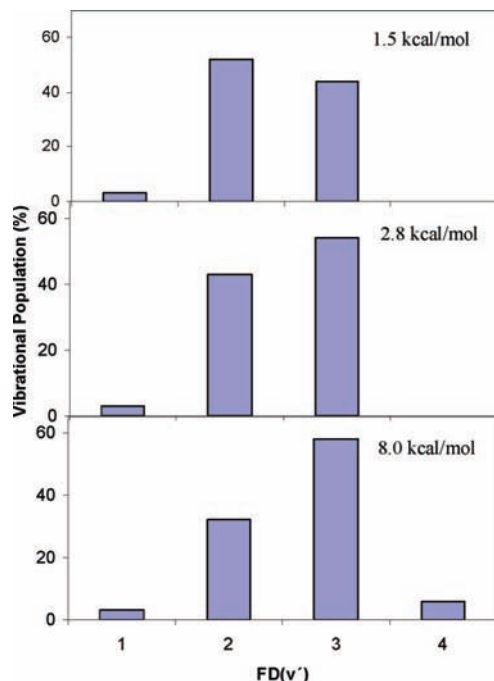


Figure 2. Vibrational state populations for the $F + \text{CHD}_3 \rightarrow \text{FD}(\nu') + \text{CHD}_2$ reaction obtained using the PES-2006 surface.

3.2. Reaction Cross Section and Product Energy Partition.

The QCT results on the PES-2006 surface at different collision energies are listed in Table 2. Most of the energy ends up in vibration of the FD product, with the amount decreasing with collision energy. This is the expected behavior that would follow from Polanyi's rules,³⁵ because the reaction proceeds via an early transition state. In this case, the reactant translation energy in excess of the barrier height is channeled mainly into product translation, $T \rightarrow T'$, and this propensity has a kinematic origin. The CHD_2 coproduct appears with a moderate amount of internal energy, 11–12% of the total available energy, independent of the collision energy. Unfortunately, there is no experimental information for comparison, but these results agree with previous QCT values obtained using the same surface for the isotopic analogues of the reaction, $F + \text{CH}_4$ and $F + \text{CD}_4$.^{5,8} For the $F + \text{CH}_4$ reaction, Zhou et al.¹⁰ reviewed the earlier experimental information and found that the energy is released mainly as vibration in the FH product and relative translation of products, with negligible internal energy in the CH_3 coproduct: $f_V(\text{FH}) = 0.61$, $f_R(\text{FH}) = 0.03$, $f_V(\text{CHD}_2) = 0.03$, $f_R(\text{CHD}_2) = 0.02$, and $f_T = 0.31$. The PES-2006 results, obtained at collision energies of 1.8 and 5.4 kcal mol⁻¹ for the $F + \text{CH}_4$ and $F + \text{CD}_4$ reactions, respectively, for direct comparison with the available experimental data, agreed qualitatively with experiment, with more internal energy in the CH_3 coproduct and less product translational energy ($f_T = 0.09$). Therefore, it seems that the PES-2006 surface and/or the QCT method underestimate the product translational energy.

Values of the state-to-state reaction cross section, σ (Å²), at three collision energies are listed in Table 3 for the $\text{CHD}_3(\nu = 0)$ reactant ground state, where only the most populated product states have been included. Experimentally, Liu et al.¹³ studied the coincident $\text{FD}(\nu')$ attributes of two coproduct states, $\text{CHD}_2(\nu_4 = 2)$ and $\text{CHD}_2(\nu_3 = 1)$, i.e., the out-of plane and scissor modes, respectively. They found that the correlated vibrational branching ratio between the $\text{CHD}_2(\nu_4 = 2)$ and $\text{CHD}_2(\nu_3 = 1)$ levels for the different $\text{FD}(\nu')$ states was very similar in the two modes and that strong variations with the

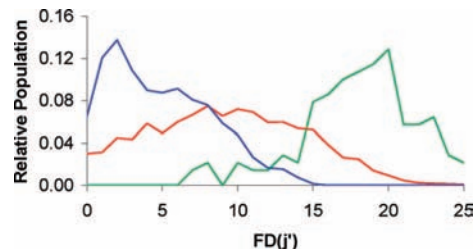


Figure 3. Discrete rotational populations for the $\text{FD}(\nu')$ product at a collision energy of 2.8 kcal mol⁻¹. The distributions are normalized so that the areas under the common levels are the same. The green, red, and blue lines correspond to vibrational states $\text{FD}(\nu' = 1-3)$, respectively.

collision energy occurred. (Note that the two states, $\nu_4 = 2$ and $\nu_3 = 1$, are practically degenerate.) Although the present theoretical study reproduces the experimental branching ratio evidence for both the $\text{FD}(\nu' = 2)$ and $\text{FD}(\nu' = 3)$ states (bold values in Table 3), it does not replicate the appreciable differences with collision energy observed experimentally.

In addition to the experimentally reported $\text{CHD}_2 \nu_3$ and ν_4 mode vibrational excitations,¹³ in the present theoretical study, we also found a vibrational excitation of the $\text{CHD}_2 \nu_6$ mode (1268 cm⁻¹). We found a population of 15–16% in the $\text{CHD}_2(\nu_6 = 1)$ mode, independent of the correlated product FD in the $\nu' = 2$ and $\nu' = 3$ states and of the three collision energies, 1.5, 2.8, and 8.0 kcal mol⁻¹. Note that this vibrational excitation percentage is practically twice that found for the $\text{CHD}_2(\nu_3 = 1)$ mode. These theoretical results are predictive, to be confirmed or rejected by future experimental measurements.

3.3. Excitation Function. The QCT total excitation function (reaction cross section versus collision energy) and the $\text{FD}(\nu')$ vibrational components are plotted in Figure 1 for the energy range 0.5–8.0 kcal mol⁻¹, where nine values of energy were used (0.5, 1.0, 1.5, 2.0, 2.8, 4.0, 5.0, 6.0, and 8.0 kcal mol⁻¹). With this surface, the threshold of the reaction is 0.35 kcal mol⁻¹, and the total reaction cross section rises rapidly from the threshold and then levels off at higher energies. There are no experimental data for comparison. However, this behavior agrees with the reported theoretical⁸ and experimental⁹ results for the analogous $F + \text{CD}_4$ reaction, indicative of a direct mechanism, but it contrasts strongly with the oscillatory pattern of the $F + \text{CH}_4$ reaction, which is associated with a quasitrapped state and is reminiscent of a signature of a reactive resonance, as has been reported experimentally⁶ and theoretically.⁷

In considering the contribution of the $\text{FD}(\nu')$ vibrational state to this function, we found that the most-populated states, $\text{FD}(\nu' = 3)$ and $\text{FD}(\nu' = 2)$, have the same tendency, i.e., the reaction cross section rises rapidly from the threshold and then levels off at higher energies. This satisfactory behavior of the PES-2006 surface in reproducing the experimental observations for two well-studied isotopic variants, CH_4 and CD_4 , lends confidence to the results reported in the present work for the $F + \text{CHD}_3$ isotopic reaction.

3.4. $\text{FD}(\nu', j')$ Product Rovibrational Distribution. Figure 2 shows the QCT $\text{FD}(\nu')$ vibrational distributions obtained using the PES-2006 surface at three collision energies. At all collision energies, there is an inversion of the $\text{FD}(\nu')$ vibrational population, with maxima for $\nu' = 2$ and 3, reproducing the experimental measurements.¹³ The population of the $\nu' = 3$ state grows with energy. At the highest energy, there is a population of 6% in the $\text{FD}(\nu' = 4)$ state.

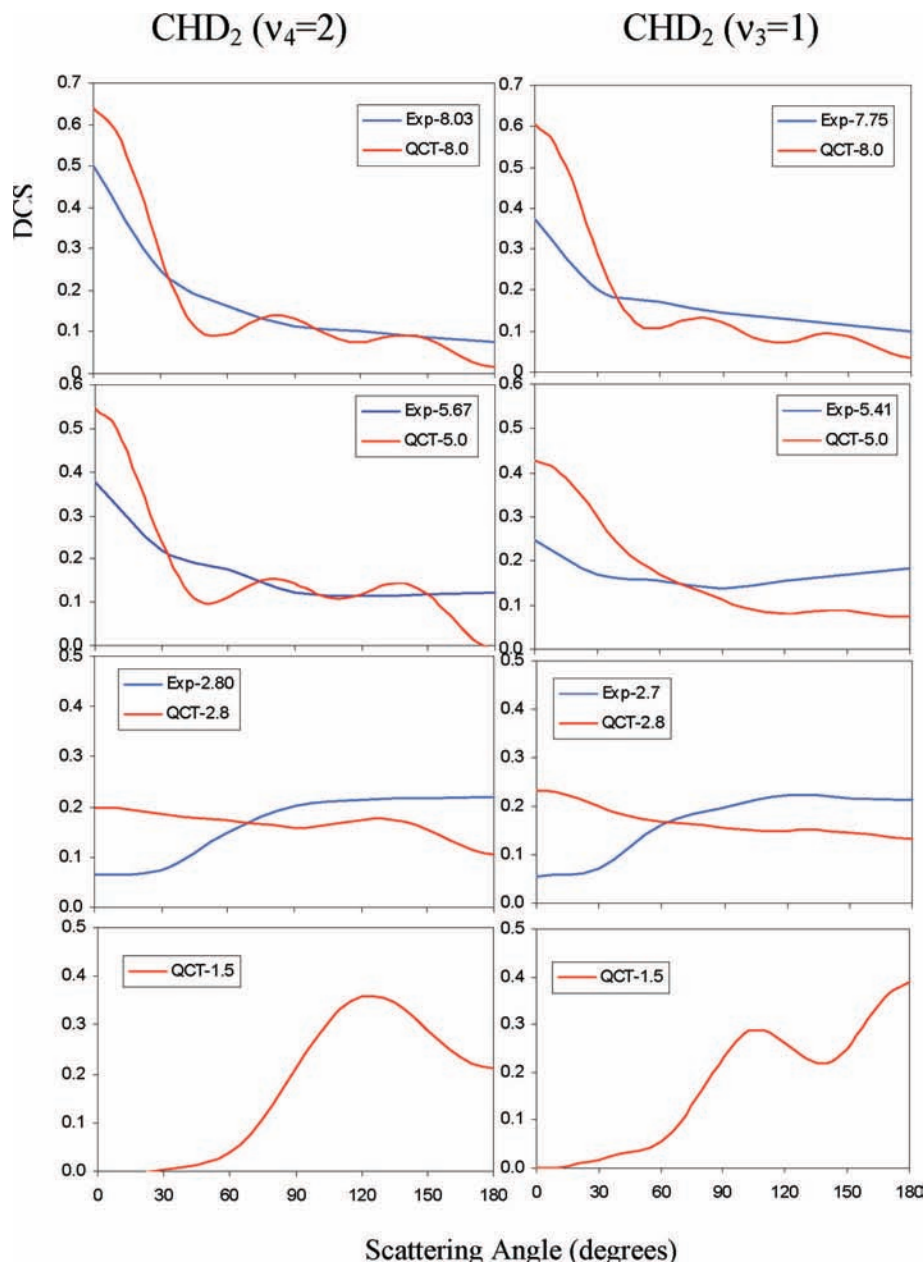


Figure 4. Theoretical and experimental product angular distributions (measured as differential cross sections, DCSs, in arbitrary units) at three collision energies considering all of the FD(ν') levels and the CHD₂($\nu_4 = 2$) and CHD₂($\nu_3 = 1$) states independently. The distributions are normalized in each plot so that the areas under the common levels are the same. Experimental values were obtained directly from Figure 6 of ref 13.

The QCT vibrationally resolved FD(ν') rotational distributions are plotted in Figure 3 for an intermediate collision energy of 2.8 kcal mol⁻¹. (For the other two energies, both lower, 1.5 kcal mol⁻¹, and higher, 8.0 kcal mol⁻¹, the rotational distributions are similar and are therefore not reproduced here.) These rotational distributions are broad and peak at $j' = 20, 10,$ and 2 for FD($\nu' = 1-3$), respectively, i.e., the rotational distributions become colder as the FD vibrational state increases. Again, there are no experimental data for comparison. However, if these rotational distributions are compared with those obtained on the same surface for the F + CH₄ reaction⁵ [which peaks at $j' = 11, 7,$ and 2 for FH($\nu' = 1-3$), respectively, reproducing the experimental information for this reaction³⁶] and the F + CD₄ reaction⁸ [which peaks at $j' = 18, 6,$ and 2 for FD($\nu' = 2-4$), respectively], this is the expected behavior. Thus, the rotational

constants are 20.77 and 10.98 cm⁻¹ for FH and FD, respectively, and consequently,³⁷ a larger rotational constant shifts j' to lower values.

3.5. Differential Cross Section (DCS). Figure 4 shows plots of the PES-2006 FD(ν') product differential scattering dynamics correlated with the coproduct CHD₂ in the $\nu_4 = 2$ and $\nu_3 = 1$ states at several collision energies, together with experimental data¹³ for comparison. (Note that, in the present work, all of the differential cross sections (DCSs) were computed by the Legendre moment method described in ref 38.) Experimentally, it was found that the DCSs evolve from backward scattering at low energy to forward scattering at high energy and that the shapes are similar for the two coproduct CHD₂($\nu_4 = 2$) and CHD₂($\nu_3 = 1$) states. The PES-2006 surface reproduces this experimental behavior, although with a collision energy about

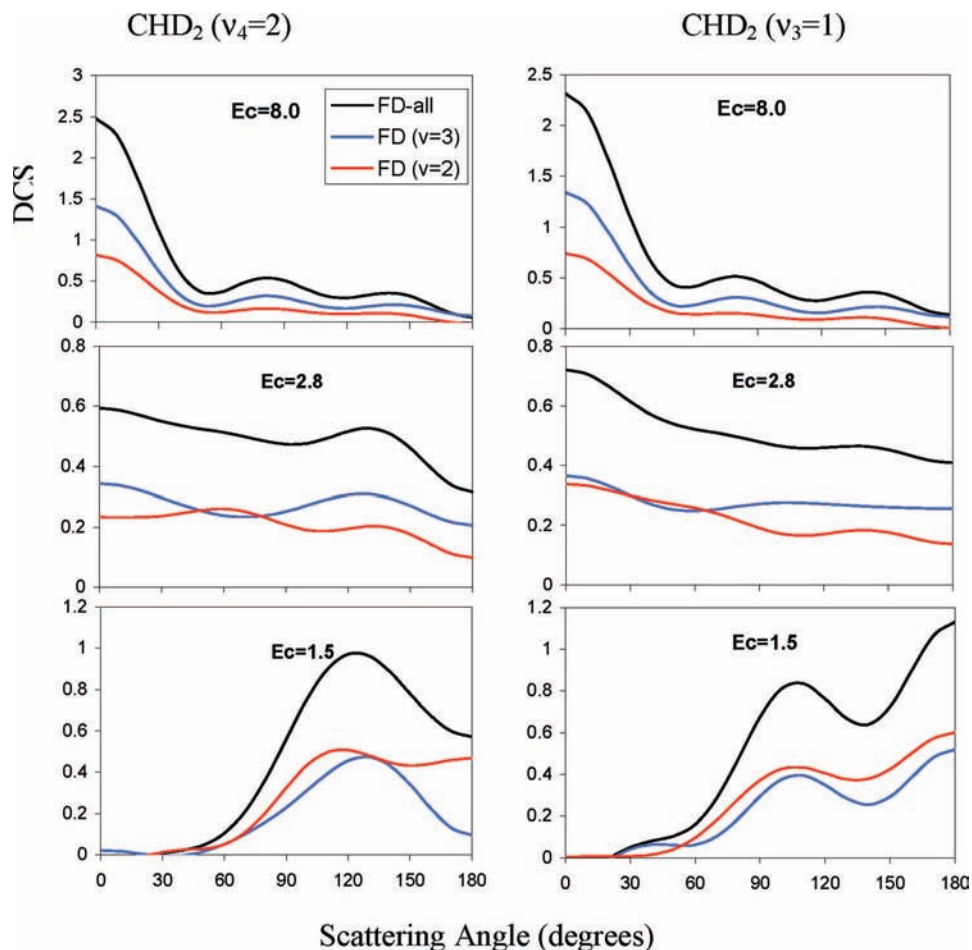


Figure 5. QCT product angular distributions (measured as differential cross sections, DCSs, in arbitrary units) at three collision energies for different vibrational FD(ν') levels correlated with the $\text{CHD}_2(\nu_4 = 2)$ and $\text{CHD}_2(\nu_3 = 1)$ states.

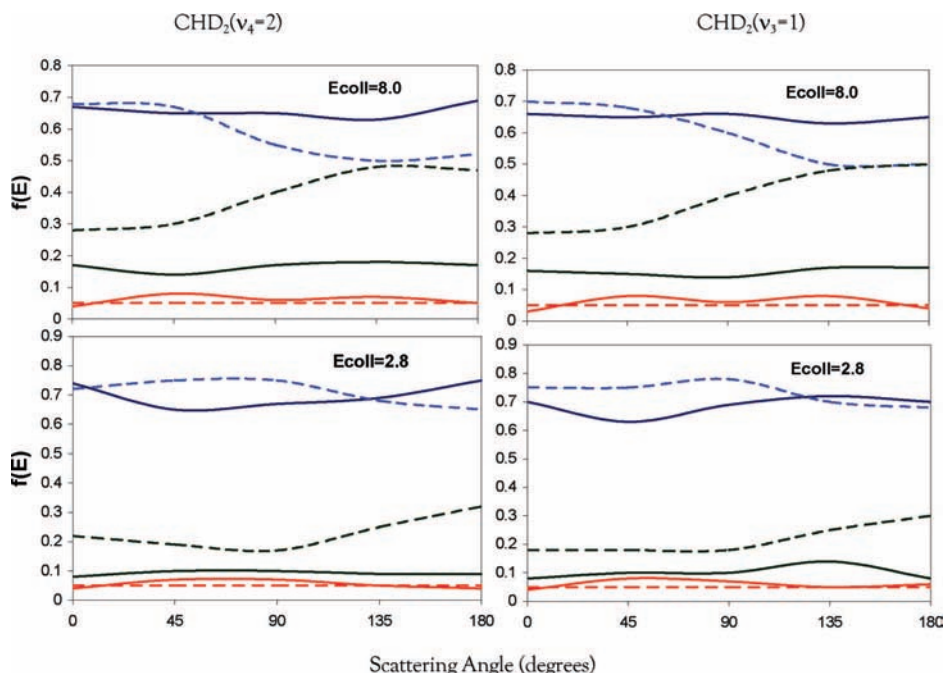


Figure 6. Correlated fractional energy disposal with the scattering angle. The blue, red, and green lines correspond to the FD vibrational energy, FD rotational energy, and product translational energy, respectively, in kcal mol⁻¹. The solid and dashed lines correspond, respectively, to the present QCT values and experimental results.¹³

1 kcal mol⁻¹ lower than experiment. Thus, the backward shape obtained experimentally at 2.8 kcal mol⁻¹ was obtained with PES-2006 at a collision energy of 1.5 kcal mol⁻¹.

This steady change of DCS with collision energy from backward to forward agrees with the behavior for the isotopic variant F + CD₄ reaction,⁸ which seems to indicate a direct mechanism for

these reactions, and is markedly different from those obtained for the analogous F + CH₄ reaction,⁵ in which dramatic changes with collision energy are observed that constitute a signature of the resonance observed experimentally by Shiu et al.⁶ and recently reported by our group⁷ using reduced-dimensionality quantum scattering calculations on the PES-2006 surface.

To analyze this behavior in more detail, Figure 5 shows plots of the QCT vibrationally state-resolved FD(ν') scattering angular distributions, again for the CHD₂($\nu_4 = 2$) and ($\nu_3 = 1$) states independently, at the three collision energies 1.5, 2.8, and 8.0 kcal mol⁻¹. At all energies and for both the CHD₂($\nu_4 = 2$) and CHD₂($\nu_3 = 1$) states, the FD vibrational contributions from the most populated states, $\nu' = 2$ and 3, reproduce the behavior of the total value, FD(ν'), in Figure 4. Thus, both FD($\nu' = 2$) and FD($\nu' = 3$) evolve steadily from backward to forward scattering as the collision energy increases. In general, these theoretical results reproduce the experimental evidence reported by Zhou et al.¹³

Finally, Figure 6 shows plots of the angular dependence of the fractional energy disposal for the CHD₂($\nu_4 = 2$) and CHD₂($\nu_3 = 1$) states independently, at the two collision energies 2.8 and 8.0 kcal mol⁻¹, together with the experimental values.¹³ At low energies, the agreement with experiment is reasonable, whereas at high energies, the agreement is poorer. In all cases, we found a more isotropic behavior of the fractional energy than experiment, although the QCT calculations reproduced the experimental results that the correlated FD rotational energy is small and practically angle-independent.

4. Conclusions

We have described an extensive state-to-state dynamics study performed using quasiclassical trajectory (QCT) calculations on an analytical potential energy surface (PES-2006) recently developed by our group for the F + CH₄ → FH + CH₃ gas-phase abstraction reaction and its isotopic analogues. In particular, we studied the isotopic variant F + CHD₃ → FD + CHD₂ reaction, with explicit consideration of the zero-point energy problem to avoid leakage along the trajectories. The collision energies ranged from 0.5 to 8.0 kcal mol⁻¹ (where the nine values of energy used were 0.5, 1.0, 1.5, 2.0, 2.8, 4.0, 5.0, 6.0, and 8.0 kcal mol⁻¹).

The abstraction of hydrogen atoms by fluorine has been a topic of long-standing interest in the chemical kinetics and molecular dynamics communities, and the FD + CHD₂ channel studied in the present work represents a specific contribution to a more global understanding of hydrogen-atom abstraction by fluorine.

Most of the available energy, 65–71%, appears as FD(ν') vibrational energy, yielding an inversion of the FD(ν') vibrational population with peaks at $\nu' = 2$ and $\nu' = 3$. The CHD₂ coproduct presented a small internal energy, just 10–12% of the available energy. The angular dependence of the fractional energy disposal for the vibrational and rotational energies of the FD product and the translational energy of products shows reasonable agreement with experiment at low energies (2.8 kcal mol⁻¹), but poorer agreement at high energies (8.0 kcal mol⁻¹).

The excitation function showed the standard behavior, rising from the threshold and then leveling off at higher energies.

In agreement with the available experimental information, we found that, in addition to excitation of the CHD₂(ν_4) umbrella mode, the CHD₂($\nu_3 = 1$) scissor mode is also vibrationally excited, with percentages of 5–9% that are similar for the correlated FD($\nu' = 2$) and FD($\nu' = 3$) states and for the three different collision energies studied. We also analyzed the product scattering distributions for these mode-correlated product pairs,

finding similar results for both CHD₂($\nu_4 = 2$) and CHD₂($\nu_3 = 1$) states, qualitatively reproducing the experimental measurements.

Finally, the comparison of the dynamics results (excitation function and evolution of the scattering distribution with collision energy) for the title reaction, F + CHD₃, with those for the analogous F + CH₄ and F + CD₄ reactions, recently reported by our group, showed that the title reaction presents a direct mechanism similar to the F + CD₄ reaction but different from the mechanism of the F + CH₄ reaction, which shows quantum resonances.

Acknowledgment. This work was partially supported by the Junta de Extremadura, Spain (Project PRI07A009).

References and Notes

- (1) Corchado, J. C.; Espinosa-García, J. *J. Chem. Phys.* **1996**, *105*, 3152.
- (2) Rangel, C.; Navarrete, M.; Espinosa-García, J. *J. Phys. Chem. A* **2005**, *109*, 1441.
- (3) Castillo, J. F.; Aoiz, F. J.; Bañares, L.; Martínez-Nuñez, A.; Fernández-Ramos, A.; Vazquez, S. *J. Phys. Chem. A* **2005**, *109*, 8459.
- (4) Troya, D. *J. Chem. Phys.* **2005**, *123*, 214305.
- (5) Espinosa-García, J.; Bravo, J. L.; Rangel, C. *J. Phys. Chem. A* **2007**, *111*, 2761.
- (6) Shiu, W.; Liu, J. J.; Lin, K. *Phys. Rev. Lett.* **2004**, *92*, 103201.
- (7) Nyman, G.; Espinosa-García, J. *J. Phys. Chem. A* **2007**, *111*, 11943.
- (8) Espinosa-García, J. *J. Phys. Chem. A* **2007**, *111*, 3497.
- (9) Lin, J. J.; Zhou, J.; Shiu, W.; Liu, K. *Science* **2003**, *300*, 966.
- (10) Zhou, J.; Lin, J. J.; Shiu, W.; Pu, S.-Ch.; Liu, K. *J. Chem. Phys.* **2003**, *119*, 2538.
- (11) Zhou, J.; Lin, J. J.; Shiu, W.; Liu, K. *J. Chem. Phys.* **2003**, *119*, 4997.
- (12) Zhou, J.; Shiu, W.; Lin, J. J.; Liu, K. *J. Chem. Phys.* **2004**, *120*, 5863.
- (13) Zhou, J.; Lin, J. J.; Liu, K. *J. Chem. Phys.* **2003**, *119*, 8289.
- (14) Porter, R. N.; Raff, L. M. In *Dynamics of Molecular Collisions*; Miller, W. H., Ed.; Plenum Press: New York, 1976; Part B.
- (15) Truhlar, D. G.; Muckerman, J. T. In *Atom-Molecules Collision Theory*; Bernstein, R. B., Ed.; Plenum Press: New York, 1979.
- (16) Raff, L. M.; Thompson, D. L. In *Theory of Chemical Reaction Dynamics*; Baer, M., Ed.; CRC Press: Boca Raton, FL, 1985; Vol. 3.
- (17) Hase, W. L.; Duchovic, R. J.; Hu, X.; Komornicki, A.; Lim, K. F.; Lu, D.-h.; Peshlherbe, G. H.; Swamy, K. N.; Van de Linde, S. R.; Varandas, A. J. C.; Wang, H.; Wolf, R. J. VENUS96: A General Chemical Dynamics Computer Program. *QCPE Bull.* **1996**, *16*, 43.
- (18) Rangel, C.; Corchado, J. C.; Espinosa-García, J. *J. Phys. Chem. A* **2006**, *110*, 10375.
- (19) Bowman, J. M.; Kuppermann, A. *J. Chem. Phys.* **1973**, *59*, 6524.
- (20) Truhlar, D. G. *J. Phys. Chem.* **1979**, *83*, 18.
- (21) Schatz, G. C. *J. Chem. Phys.* **1983**, *79*, 5386.
- (22) Lu, D.-h.; Hase, W. L. *J. Chem. Phys.* **1988**, *89*, 6723.
- (23) Varandas, A. J. C. *Chem. Phys. Lett.* **1994**, *225*, 18.
- (24) Ben-Nun, M.; Levine, R. D. *J. Chem. Phys.* **1996**, *105*, 8136.
- (25) McCormack, D. A.; Lim, K. F. *Phys. Chem. Chem. Phys.* **1999**, *1*, 1.
- (26) Stock, G.; Müller, U. *J. Chem. Phys.* **1999**, *111*, 65.
- (27) Marques, J.M.C.; Martínez-Nuñez, E.; Fernández-Ramos, A.; Vazquez, S. *J. Phys. Chem.* **2005**, *109*, 5415.
- (28) Duchovic, R. J.; Parker, M. A. *J. Phys. Chem.* **2005**, *109*, 5883.
- (29) Bonnet, L.; Rayez, J. C. *Chem. Phys. Lett.* **1997**, *183*, 277.
- (30) Bonnet, L.; Rayez, J. C. *Chem. Phys. Lett.* **2004**, *397*, 106.
- (31) Shimanouchi, T. *Molecular Vibrational Frequencies*. In *NIST Chemistry WebBook, NIST Standard Reference Database Number 69*; Linstrom, P. J., Mallard, W. G., Eds.; National Institute of Standards and Technology (NIST): Gaithersburg, MD, 2005; p 20899.
- (32) Mebel, A. M.; Lin, S.-H. *Chem. Phys. Lett.* **1997**, *215*, 329.
- (33) Brum, J. L.; Johnson, R. D.; Hudgens, J. W. *J. Chem. Phys.* **1993**, *98*, 3732.
- (34) Spanbauer, R. N.; Rao, K. N. *J. Mol. Spectrosc.* **1965**, *16*, 100.
- (35) Polanyi, J. C. *Science* **1987**, *236*, 680.
- (36) Harper, W. H.; Nizkorodov, S. A.; Nesbitt, D. J. *J. Chem. Phys.* **2000**, *113*, 3670.
- (37) In the rigid rotor model, the maximum of the j number and the rotational constant, B , are related by the expression $j_{\max} = (K_b T / 2B)^{1/2} - 1/2$, where K_b and T are the Boltzmann constant and the temperature, respectively.
- (38) Truhlar, D. G.; Blais, N. C. *J. Chem. Phys.* **1977**, *67*, 1532.